Functional Near Infrared Spectroscopy (NIRS) signal improvement based on negative correlation between oxygenated and deoxygenated hemoglobin dynamics

Xu Cui[1,2,*], **Signe Bray**[1,2], and **Allan L. Reiss**[1,2]

[1] Department of Psychiatry and Behavioral Sciences, School of Medicine, Stanford University, 401Quarry Road, Stanford, CA 94305, USA

[2] Center for Interdisciplinary Brain Sciences Research, Stanford University, 401Quarry Road, Stanford, CA 94305, USA

Abstract

Near infrared spectroscopy (NIRS) is a promising technology for functional brain imaging which measures hemodynamic signals from the cortex, similar to functional magnetic resonance imaging (fMRI), but does not require the participant to lie motionless in a confined space. NIRS can therefore be used for more naturalistic experiments, including face to face communication, or natural body movements, and is well suited for real-time applications that may require lengthy training. However, improving signal quality and reducing noise, especially noise induced by head motion, is challenging, particularly for real time applications. Here we study the properties of head motion induced noise, and find that motion noise causes the measured oxygenated and deoxygenated hemoglobin signals, which are typically strongly negatively correlated, to become more positively correlated. Next, we develop a method to reduce noise based on the principle that the concentration changes of oxygenated and deoxygenated hemoglobin should be negatively correlated. We show that despite its simplicity, this method is effective in reducing noise and improving signal quality, for both online and offline noise reduction.

Introduction

Near infrared spectroscopy (NIRS), a non-invasive optical imaging method that measures concentration change of hemoglobin *in vivo*, is an increasingly popular tool for functional neuroimaging. NIRS has several advantages over functional magnetic resonance imaging (fMRI), including low cost, portability, quietness, and higher temporal resolution. Like fMRI, NIRS can be used to measure the hemodynamic response during neural activity, and the data can be analyzed post-hoc or in real time (e.g. for neurofeedback and BCI studies).

NIRS measurement probes are typically affixed to the surface of the head using a cap. Since NIRS does not require the participant to lie in a confined, noisy space, it can theoretically be used for more ecologically valid paradigms, and for experiments with individuals who do not tolerate the MRI scanner environment, including children and clinical populations. However,

*Corresponding author. cuixu@stanford.edu, Tel: 607-229-6538, Center for Interdisciplinary Brain Sciences Research, Department of Psychiatry and Behavioral Sciences, Stanford University, 401 Quarry RD, Stanford, CA 94305, US.

there exists a tradeoff between ecological validity and signal quality: in situations where the subject's head is totally unrestrained, motion induced noise is more likely to degrade signal quality.

NIRS is significantly more tolerant of head motion than fMRI and has been used in experiments in which subjects make large movements (e.g. exercise or driving). However, NIRS is not impervious to subject-motion induced noise. When subjects move, the NIRS optodes may shift relative to the head and alter the coupling between source and scalp, and detector and scalp, and may also change the distance between source and detector. This results in an artifact that changes abruptly with the motion, potentially inducing spikes with amplitude much larger than the true signal.

Failure to adequately correct for motion induced noise may lead to biased or false conclusions. This problem is exacerbated in real-time neurofeedback studies, in which motion induced signal change may be falsely attributed to neural events. Motion correction algorithms applied post-hoc typically use signal values across the entire recording to infer which segments have been contaminated by noise. In contrast, motion correction in real-time applications must make adjustments to the current time point based only on current and past values. In this situation, spike detection algorithms based on thresholding are impractical, because some motion interference will be on the same scale as true signal change, and because time points surrounding the peak of a spike also include sub-threshold motion-induced noise that will not be corrected.

A growing number of algorithms are being developed for NIRS noise reduction and signal improvement. There are three types of noise in NIRS data, the instrument noise, the physiological noise and experiment error (including head motion). Existing noise reduction approaches can be categorized into three general categories: (1) reducing noise based on its *temporal* characteristics, (2) reducing noise based on its *spatial* characteristics, and (3) measuring noise independently and subtracting it from the signal. The first category includes methods such as band pass filtering, moving averaging, and Wiener filtering and can effectively eliminate high frequency instrument noise and low frequency drift. Unfortunately, this class of algorithms usually fails to remove abrupt spike-like noise. Algorithms in the second category, for example, eigenvector based algorithms, usually assume that signal due to noise is broadly spatially distributed compared to signal due to neural activity. However, with eigenvector based methods one often needs to make subjective decisions about the number of components to keep, and they are difficult to apply to real-time processing. In the third category, noise is measured independently by additional hardware. For example, head motion can be measured using an accelerometer, or noise can be measured using a channel with a very short distance between the emitter and detector so that the infrared light doesn't pass through the brain tissue. The resultant signal must be noise, which can be subtracted from the signal. This class of methods requires additional hardware, which is often not available in existing commercial NIRS devices.

NIRS is unique among imaging technologies to simultaneously measure the concentration changes of oxygenated and deoxygenated hemoglobin (oxy-Hb and deoxy-Hb). Here we propose a simple noise reduction method designed to exploit the statistical association between these measures during brain activation. Many studies have established that oxy-Hb and deoxy-Hb concentration are negatively correlated during neural activation. For example, during a finger tapping task, oxy-Hb in contralateral motor cortex usually increases and deoxy-Hb usually decreases, though the amplitude of deoxy-Hb is often smaller than that of oxy-Hb. We propose to remove noise from NIRS signals based on the rationale that if the measured oxy-Hb and deoxy-Hb signals are not strongly negatively correlated, it's likely that the signals contain substantial noise.

In this study, we investigate the effect of head motion on NIRS data and develop a method to reduce noise. In Experiment 1, we use both Balloon model simulations of NIRS measurements and empirical data recorded during a block-design finger tapping task, with different amounts of head motion, to investigate the effect of head motion on NIRS signal quality. We find that oxy- and deoxy-Hb are strongly negatively correlated and that motion causes the correlation between oxy- and deoxy-Hb to become more positive. In Experiment 2, we develop a method for improving NIRS signal based on the principle that the true oxy-Hb and deoxy-Hb signals should be negatively correlated. We demonstrate that this method, when used for post-experimental (offline) analysis or real time (online) applications, is effective at removing large spike-like noise and improving signal quality.

Experiment 1: Investigating the properties of motion-induced noise in NIRS

Methods

Participants—Ten healthy young adults (mean age 26.9, age range 22–37, 4 males) participated in this study. Three participants had black hair, while the remaining seven had brown hair. Written informed consent was obtained from all subjects, and the study protocol was approved by the Stanford University Institutional Review Board.

Experimental procedure—This experiment consisted of 3 blocks and lasted about 15 minutes in total. The blocks were labeled "finger tapping only" (FO), "finger tapping with *small* head motion" (FS) and "finger tapping with *big* head motion" (FB). The three blocks were performed in series with no breaks and no change of NIRS cap position on the head. For the first five participants, the order of blocks was always FO-FS-FB; for the second five participants, block order was randomized.

The task consisted of 10 seconds of finger tapping alternating with 20 second rest periods. Each participant completed 10 periods of tapping in each of the FO, FS and FB blocks. Before the experiment, participants were asked to sit relaxed and let their right hand rest naturally on their right knee. When the word "Tap" appeared on the screen, they began tapping all four fingers on their right hand at a rate of 3–4 taps per second. When "xxx" appeared on the screen, they stopped tapping.

During the FS and FB blocks, in addition to tapping, participants were asked to make single head motions following cues presented on-screen. In the FS block, the instructions were "forward small", "left small", "backward small" and "right small". Each motion instruction occurred 10 times, on average every 9s (1s standard deviation), asynchronous with the alternating finger tapping and rest blocks. The first word indicated the direction in which the participants should move their heads. In the FB block, the instructions were "forward big", "left big", "backward big" and "right big" and each occurred 10 times. For "big" head motions, subjects participants were asked to move their head as far as possible without moving their shoulders; for "small" head motions, they were asked to move half way. Participants were asked to move their head at a natural speed (~ 3–4 seconds for a big head motion and 1–2 seconds for a small motion).

During the FS and FB blocks, the participants followed two instructions in parallel, one for finger tapping and one for head motion, and thus, it may have been difficult for some subjects to attend to both sets of visual instructions. To overcome this potential problem, an auditory signal (beep) was provided that was temporally coincident with the "Tap" and "xxx" instructions. Thus, participants could use the auditory signals as an indicator of tapping onset and offset.

We observed participants' performance during the entire experiment. They followed the instructions correctly: head motion was minimal during FO block, and larger in the FB block than in the FS block.

Before the experiment, each participant practiced all 3 blocks of the task for 5–10 minutes to make sure that they understood the instructions and performed the task correctly.

NIRS data acquisition and processing—We used an ETG-4000 (Hitachi, Japan) Optical Topography system to measure the concentration change of oxy-Hb and deoxy-Hb. We used the two "4×4" measurement patches provided by Hitachi. The two patches were attached to a regular swimming cap. In each patch, 8 emitters and 8 detectors are positioned alternatingly, for a total of 32 probes, resulting in 48 measurement channels. The sampling frequency was 10Hz. The measurement area covered bilateral motor cortex, as we expected the left motor cortex to be activated by the right finger tapping task.

Band pass filtering—For offline data processing, band pass filtering was applied to the raw data before any further processing (including the offline version of the noise reduction method developed here). High frequency instrument noise and low frequency drift in oxy-Hb and deoxy-Hb signal were removed using band pass filtering with cutoff frequencies of 0.01 and 0.5Hz.

Running Correlation (RC)—We calculated the running correlation (RC) to access the correlation between oxy-Hb and deoxy-Hb at each time point. RC at time point t is defined as the correlation between segments of oxy-Hb and deoxy-Hb in the time window between t-w and t+w, where w is the half window size. We used w=50 (5s) in our calculations, except at the beginning and end of the signal, where the half window size was adjusted so that the segment was symmetric around time point t.

Balloon model simulation—We used the balloon model to simulate the true oxy-Hb and deoxy-Hb signal without noise. The balloon model is a biomechanical model of hemodynamics during brain activation that shows strong agreement with experimental measurements. We used the same differential equation as Mildner et al. (Equation 11 in their paper) with an additional equation describing the dynamics of the total hemoglobin concentration (total-Hb = oxy-Hb + deoxy-Hb):

$$\dot{q}(t) = \frac{f_{in}(t)}{\tau_0}\left[\frac{E(t)}{E_0} - \frac{q(t)}{v(t)}\right] + \frac{1}{\tau_v}\left[f_{in}(t) - v^{1/\alpha}\right]\frac{q(t)}{v(t)}$$
$$\dot{v}(t) = \frac{1}{\tau_v}\left[f_{in}(t) - v^{1/\alpha}\right]$$
$$\dot{p}(t) = \frac{1}{\tau_v}\left[f_{in}(t) - v^{1/\alpha}\right]\frac{p(t)}{v(t)}$$

where q, v, and p denote deoxy-Hb, blood volume, and total-Hb respectively. Oxy-Hb is obtained by subtracting deoxy-Hb from total-Hb. The blood inflow *fin* is modeled as a trapezoidal function with rise time 5s, plateau time 5s, decay time 5s and plateau height 1.7. The oxygen extraction factor E is modeled as $E = 1 - (1-E0)^{1/fin}$ with E0 is 0.4. Other parameter values are: $\tau_0 = 2$, τ_v=30, α=0.4, similar to Mildner et al.

Results

Simulated oxy-Hb and deoxy-Hb are negatively correlated—To find the correlation between true oxy-Hb and deoxy-Hb without noise, we simulated the dynamics of oxy-Hb and deoxy-Hb using the balloon model and calculated the running correlation between them. Figure 1 shows the dynamics of oxy-Hb and deoxy-Hb. Following blood inflow as a consequence of neural activation, oxy-Hb concentration increases and deoxy-Hb decreases. The correlation

between oxy-Hb and deoxy-Hb is negative and close to -1. During the plateau period, the correlation becomes less negative. Overall, true oxy-Hb and deoxy-Hb are negatively correlated – when one increases, the other should decrease.

Measured oxy-Hb and deoxy-Hb are negatively correlated—In the absence of head motion in the finger tapping only block (FO), the signal we measured is as close as possible to the true oxy-Hb and deoxy-Hb. Following preprocessing (e.g. bandpass filtering) we calculated the running correlation (RC) between oxy-Hb and deoxy-Hb for channel 13 (corresponding to the left motor cortex) on a single subject (Figure 2a) during the finger tapping only task (FO). We found that the correlation between measured oxy-Hb and deoxy-Hb is largely negative and close to −1 most of the time, and that this is generally the case for all channels (Figure 2b, c).

Head motion induced noise causes a positive shift of the correlation—What is the effect of head motion on the correlation between oxy-Hb and deoxy-Hb? In Figure 3 we show the correlation between oxy-Hb and deoxy-Hb in a single subject for the three levels of head motion. We observe that head motion makes the correlation higher (less negative), larger head motion causes higher (positive) correlation than small head motion, and the correlation increase is not uniform across channels (e.g. channel 24 overlying the left parietal cortex is particularly susceptible).

The raw signal is not obviously degraded for the smaller amount of head motion (FS; Figure 3b). This is in contrast to fMRI data which would be virtually unusable with this amount (~10cm) of head motion. Quantitatively, after removing the finger tapping related signal from oxy-Hb by narrowing the band pass filter (i.e. keeping components with frequency > 0.1 Hz, where the finger tapping related signal has a frequency 0.033 Hz), the residual (considered to be noise) has standard deviation of 0.03 (FO block), 0.03 (FS block) and 0.07 (FB block). The noise level in oxy-Hb is similar in the FS and FO blocks. This also implies that the correlation between oxy- and deoxy-Hb is more sensitive to head motion than the noise level in either oxy- or deoxy-Hb signal alone and amplitude based signal improvement procedures may be inadequate for correcting more subtle motion induced noise.

We calculated the positive shift of the correlation due to head motion for all participants (Figure 3g). The mean increase of running correlation from FO block to FS block is 0.52 (Paired t-test, df=9, p=3×10^{-6}) across subjects; the increase from FO block to FB block is 0.97 (p=2×10^{-8}).

Experiment 2: Development of a correlation based signal improvement method

In Experiment 1 we established that under ideal conditions, oxy-Hb and deoxy-Hb should be maximally negatively correlated, and that head-motion induced noise causes the correlation to become more positive. In Experiment 2, we develop a method for noise reduction that is based on maintaining a negative correlation between oxy-Hb and deoxy-Hb, and apply this method to the noisy data collected in Experiment 1.

Methods

Development of Correlation Based Signal Improvement (CBSI) method—Assume the measured signal of oxy-Hb and deoxy-Hb has three components: (1) the true signal which we endeavor to estimate, (2) noise that has identical effects on oxy-Hb and deoxy-Hb (e.g. head motion induced noise) subject to a constant factor, and (3) other white noise. Let x, y, x_0 and y_0 be measured oxy-Hb, measured deoxy-Hb, true oxy-Hb, and true deoxy-Hb, respectively. We then have,

$$x = x_0 + \alpha F + Noise$$
$$y = y_0 + F + Noise \tag{1}$$

where F is noise which has identical effects on oxy-Hb and deoxy-Hb subject to a positive constant factor a. Note that x, y, x_0, y_0 and F are all functions of time t. The "*Noise*" term in the equation is usually high frequency white noise introduced by the NIRS device. Contrary to F, this type of noise fluctuates independently in oxy- and deoxy-Hb signal. This white noise can be effectively removed by standard filtering techniques so we exclude this term in future derivations. As F is external, we also assume F is independent from the true signal x_0 and y_0. We further assume that the signal has been offset corrected to have zero mean.

Our goal is to find x_0 and y_0 subject to two assumptions:

1. x_0 and y_0 should be maximally negatively correlated (close to -1)

2. x_0 and F should be minimally correlated (close to 0)

Assume assumption (1) is satisfied, we can express the relationship between x_0 and y_0 as

$$x_0 = -\beta y_0$$

where β is a free parameter accounting for the amplitude difference between oxy-Hb and deoxy-Hb. By inserting this equation to equation (1), we can find,

$$F = \frac{1}{\alpha+\beta}(x+\beta y)$$
$$x_0 = \frac{\beta}{\alpha+\beta}(x - \alpha y)$$

Then we apply the second assumption that F and x_0 should be minimally correlated. If we set the correlation between F and x_0 to zero, we get

$$\sum_t x^2 + (\beta - \alpha)\sum_t xy - \alpha\beta\sum_t y^2 = 0$$

We want to solve for α and β, but there are an infinite number of solutions of this equation. At this point, let's examine the meaning of α and β. α is the ratio of the noise amplitude in oxy-Hb and deoxy-Hb, and β is the ratio of the amplitude of true oxy-Hb and deoxy-Hb. In empirical data (e.g. the data in Figure 4a below), we often observe that deoxy-Hb has smaller amplitude than oxy-Hb, and at the same time the spikes (noise) caused by head motion in deoxy-Hb are proportionally smaller than the spikes in oxy-Hb. It is therefore reasonable to start with the assumption that $\alpha=\beta$. While this assumption is based on empirical data rather than theory, we feel that this assumption is justified by the fact that the resultant method is efficient at removing head motion induced noise.

With $\alpha=\beta$, we have

$$\alpha = \sqrt{\frac{\sum x^2}{\sum y^2}} = \frac{std(x)}{std(y)}$$

Thus we reach a very simple result,

$$x_0 = \frac{1}{2}(x - \alpha y)$$
$$y_0 = -\frac{1}{\alpha} x_0$$

(2)

where α is the ratio of the standard deviation of measured oxy-Hb and deoxy-Hb signal.

We call this method "Correlation Based Signal Improvement" (CBSI) method for later reference. The corrected signal is simply a linear combination of measured oxy-Hb and deoxy-Hb signals and we call it the "corrected activation signal".

Real-time extension of CBSI method—The CBSI method we developed here has three characteristics that make it ideal for real time signal quality improvement: (1) correction at time t doesn't require data to be collected later than t, (2) the method is simple and the computational cost is low, and (3) it can be implemented as an automated algorithm and does not require user intervention.

We investigated the performance of the real-time CBSI method on the data collected in Experiment 1, with the constraint that no future data points can be used to correct signal at the current time point. We first used an exponential moving average (EMA) filter (see below) instead of band pass filtering to remove high and low frequency noise from the data, and used a window of 100s to calculate a from the standard deviation of oxy-Hb and deoxy-Hb.

Exponential moving average (EMA)—EMA is a real-time method to remove high frequency noise and low frequency drift from the signal and can be viewed as an online version of band pass filtering. EMA computes the long-term (L) and short-term (S) moving average of a time series and outputs the difference between them. EMA effectively eliminates the low- and high-frequency components from the original signal with low computational cost. Specifically, assume the original signal is $f(t)$ and the filtered signal is $g(t)$, then

$$L(t) = \frac{1}{\alpha_L} f(t) + (1 - \frac{1}{\alpha_L}) L(t-1)$$
$$S(t) = \frac{1}{\alpha_S} \sum_{k=0}^{\alpha_S} f(t-k)$$
$$g(t) = S(t) - L(t)$$

where $L(1) = f(1)$, $\alpha_L = 100$ and $\alpha_S = 20$. The sampling frequency is 10Hz and that means our short term moving average has a window of 2s.

Contrast-to-noise-ratio (CNR)—We use contrast-to-noise-ratio (CNR) to quantify the signal to noise ratio. Basically, CNR calculates the amplitude difference between the signal during finger tapping and the signal during rest, divided by the pooled standard deviation. Larger CNR indicates that the ratio of finger tapping related signal to noise is larger.

$$CNR = \frac{mean(dur) - mean(pre)}{\sqrt{\mathrm{var}(dur) + \mathrm{var}(pre)}}$$

"dur" means during finger tapping, and "pre" means the rest period before finger tapping. Considering the hemodynamic delay, we chose a time window between 6–12s after the beginning of tapping as "dur" and 0–5s before finger tapping as "pre".

As deoxy-Hb decreases during activation, the resultant CNR is negative. For deoxy-Hb analyses we flip the sign of the CNR for easier comparison with oxy-Hb.

Results

The CBSI method effectively removes spikes—We applied the CBSI method to our data and found that spikes are effectively removed. Figure 4a shows the original oxy-Hb (red) and deoxy-Hb (blue) time series and the corrected activation (black) time series from a single channel (channel 24) in subject 4. The large spikes visually evident in the original signal are largely removed by the CBSI method. Figure 4b and 4c show the original oxy-Hb time series and corrected activation time series for all channels in subject 4, side by side. The spikes in channels 20–25 and 44–48 are largely removed.

The CBSI method improves signal quality—The CBSI method not only removes spikes with large amplitude, it also reduces non-spike noise and improves signal quality. Figure 5a shows the original oxy-Hb time series (red) and corrected activation time series (black) in channel 13 from subject 4. In the original times series, it's difficult to tell whether or not the signal is correlated with the finger tapping task on a single trial basis. After correction, it's clear that the signal follows finger tapping. The contrast to noise ratio after correction (CNR) is 2.59, compared to 1.31(oxy-Hb) and 1.28 (deoxy-Hb) before correction.

Figure 5b-d shows the CNR before and after correction for all 10 participants. We functionally localized the left motor cortex by identifying the channel with the highest CNR among all channels in the FO block for each subject, and then computed the CNR on oxy-Hb and deoxy-Hb before and after correction in this channel for the FB block for each subject (Figure 5b). Note that the corrected activation signal for oxy-Hb is perfectly anti-correlated with that of deoxy-Hb (Equation 2), and therefore the CNR of the corrected deoxy-Hb activation signal is identical to oxy-Hb. CNR is improved in 9 of the 10 participants for oxy-Hb and in all 10 participants for deoxy-Hb. For oxy-Hb, the mean increase is 0.80 (one tailed paired t-test, df=9, p $=8\times10^{-4}$); for deoxy-Hb, the mean improvement is 0.89 (one tailed paired t-test, df=9, p $=4\times10^{-4}$). For data with less noise, as in the FO and FS blocks, the mean improvement is still positive but small in size (e.g. 0.17 for oxy-Hb in FO block) (Figure 5cd). This indicates that the CBSI method significantly improves data with a large amount of noise, and at the same time doesn't degrade data quality for data with a small amount of noise.

The CBSI method improves spatial specificity—A good signal improvement algorithm should recover the true signal from the measured signal. As a consequence, CNR of the active region should increase (in this case left motor cortex for the right-finger tapping task), and the CNR of nonspecific regions should decrease (such as channels in the right hemisphere). Here we investigated the CNR in all channels for a single subject (#4). Figure 6 shows the CNR map of the original oxy-Hb signal (a) and corrected activation signal (b) in the FB block. For comparison, the original oxy-Hb CNR map in the FO block is shown in Figure 6c. The CBSI method improved the localization of the activation map to a level comparable to data without head motion.

CBSI method for real time signal processing—The simplicity of the CBSI method makes it ideal for real time noise reduction. We found the real-time version of the CBSI method works similarly to the offline version, as demonstrated on the data of an individual participant (subject 4). Figure 7a shows that the real time CBSI method can effectively remove spikes, and improves signal quality in motor cortex (Fig 7b). The corrected signal is more clearly correlated with finger tapping than the uncorrected signal.

The real-time implementation of the CBSI method requires the choice of a window size for calculating the standard deviation. We tried several different time windows and the results are basically unchanged as long as the window is reasonably large (>30s).

Discussion

We have developed a correlation based signal improvement (CBSI) method that can be used online or offline in NIRS data analysis. The method is based on the assumption that true oxy-Hb and deoxy-Hb should be maximally negatively correlated. We have shown that this method can effectively remove large spikes caused by head motion and improve signal quality and spatial specificity.

Compared to existing noise reduction methods, the CBSI method has several advantages. First, the method is simple and does not require advanced mathematical knowledge: the corrected signal is simply a linear combination of oxy-Hb and deoxy-Hb. Our implementation of the CBSI method is available at http://www.alivelearn.net/nirs/CBSI.m. Second, the CBSI method is fully automated; the offline version does not have any free parameters and thus does not require any arbitrary parameter choices. For the online (real-time) version, there is only one free parameter to be decided - the time window which is used to estimate standard deviation of oxy-Hb and deoxy-Hb – and the performance of the method is not sensitive to this window size. Third, the CBSI method can be applied for both offline and online signal processing, as it only requires the current and past signal values, and the computational cost is low. Lastly, the method is blind to the experimental paradigm and doesn't require information such as event onset timing.

Our method is based on the assumption that oxy-Hb and deoxy-Hb are negatively correlated. This has been justified by numerous independent studies and by our own data. However, while our method assumes that oxy-Hb and deoxy-Hb are *perfectly* negatively correlated, this is not true in practice. As Figure 1 shows, the correlation is less negative during the plateau period. It is also likely that the correlation is more complicated during the "overshooting" and controversial "initial dip" phases of the hemodynamic response. As a consequence, the corrected signal estimated by the CBSI method might be different from the true signal. While this is true, we propose that our approach is a reasonable approximation. First, as we have seen in Figure 2, the correlation of oxy-Hb and deoxy-Hb is typically close to −1. Second, the time period during which the oxy-Hb and deoxy-Hb correlation deviates from −1 is usually when they don't change (at baseline or plateau), and we are more interested in signal change during activation. Third, a method based on the assumption of a dynamic correlation is technically difficult to develop, and would likely require introducing free parameters or information about the experimental paradigm (e.g. event onset timing). However, it is likely that such a method could improve the signal quality even further.

Our method is developed based on data from healthy young adults performing a (right) finger tapping experiment which activates the (left) motor cortex area. The effectiveness of this method in other brain areas and other experiment paradigms needs to be investigated in the future. However, it's likely that this method is generally effective in functional NIRS data for two reasons. First, as shown in Figure 4, spikes are effectively removed in channels 20–24 and 44–48, which corresponds to parietal cortex and temporal cortex. Second, the theoretical basis

and the derivation of the method are based on general properties of NIRS (e.g. negative correlation between oxy- and deoxy-Hb) which are largely independent of any particular brain region or experiment.

Most neuroimaging experiments are performed in highly artificial environments: subjects are asked to refrain from moving, confined in small spaces, communicate by button box rather than by speech, view images on computer screens rather than real stimuli, and repeat the same experiment trials many times. These deeply artificial experimental settings don't reflect the real environment to which human beings need to adapt. To this end, NIRS is a more optimal technology for performing ecologically valid experiments. However, there is a trade-off between data quality and the naturalness of experiments. In fMRI studies the head is often restrained, which helps reduce motion artifact. During NIRS studies, we have the option of including tasks that involve more motion on the part of the subject, but this may be at the expense of data quality. While this method and others have been developed to improve NIRS signal quality, acquisition of good signal in the first place is always preferred. As mentioned above, optode shift following head movement is believed to be the main cause of abrupt noise. As a consequence, increasing the stability of optodes on the head surface is extremely important to obtain high quality data. We used a swimming cap to hold the optode grid against the head, which is effective at maintaining the position of the optodes when head motion is small or slow. However, when head motion is large, more sophisticated head gear would be useful to stabilize the optodes. In addition to better head gear, one needs to minimize the factors which may potentially contribute to optode shift. A few good practices we use are: 1) Minimize the tension on the optical fibers. The fibers should not pull the probes; instead, they should hang naturally. 2) Try to create a comfortable setting for the participants (e.g. a comfortable chair with suitable height, suitable position of button box or keyboard, and reasonable duration of experiment etc.). Participants are more likely to move when they are uncomfortable. 3) Avoid settings which facilitate unnecessary movement (e.g. a bouncy or swivel chair).

In this study we investigated the correlation of oxy- and deoxy-Hb under ideal conditions and under varying amounts of head-motion induced noise. We found that while oxy- and deoxy-Hb are generally negatively correlated, head motion causes the correlation to become more positive. This finding was then used to develop a method for signal improvement that is based on maximizing the negative correlation between the two signals. We show that this method removes spikes, improves the contrast-to-noise ratio during a finger-tapping task, and improves spatial specificity. This method is well suited to real-time applications, and we show that the CBSI method works well for real-time signal correction. While this method improves signal with large amounts of noise, we also show that it does not degrade signal quality in situations with minimal noise, making this a simple step that could be included in any NIRS preprocessing pipeline.

Acknowledgments

References

1. Abdelnour A, Huppert T. Real-time imaging of human brain function by near-infrared spectroscopy using an adaptive general linear model. NeuroImage 2009;46:133–143. [PubMed: 19457389]

2. Bauernfeind G, Leeb R, Wriessnegger SC, Pfurtscheller G. Development, set-up and first results for a one-channel near-infrared spectroscopy system. Biomedizinische Technik. Biomedical engineering 2008;53:36–43. [PubMed: 18251709]

3. Boas DA, Strangman G, Culver JP, Hoge RD, Jasdzewski G, Poldrack RA, Rosen BR, Mandeville JB. Can the cerebral metabolic rate of oxygen be estimated with near-infrared spectroscopy? Physics in medicine and biology 2003;48:2405–18. [PubMed: 12953906]

4. Buxton RB, Uludag K, Dubowitz DJ, Liu TT. Modeling the hemodynamic response to brain activation. Neuroimage 2004;23(Suppl 1):S220–33. [PubMed: 15501093]

5. Buxton RB, Wong EC, Frank LR. Dynamics of blood flow and oxygenation changes during brain activation: the balloon model. Magnetic resonance in medicine 1998;39:855–64. [PubMed: 9621908]

6. Buxton RB, Frank LR. A model for the coupling between cerebral blood flow and oxygen metabolism during neural stimulation. J Cereb Blood Flow Metab 1997;17:64–72. [PubMed: 8978388]

7. Coyle SM, Ward TE, Markham CM. Brain-computer interface using a simplified functional near-infrared spectroscopy system. Journal of neural engineering 2007;4:219–26. [PubMed: 17873424]

8. Devor A, Dunn AK, Andermann ML, Ulbert I, Boas DA, Dale AM. Coupling of total hemoglobin concentration, oxygenation, and neural activity in rat somatosensory cortex. Neuron 2003;39:353–9. [PubMed: 12873390]

9. Huppert TJ, Diamond SG, Franceschini MA, Boas DA. HomER: a review of time-series analysis methods for near-infrared spectroscopy of the brain. Applied optics 2009;48:D280–98. [PubMed: 19340120]

10. Ide K, Secher NH. Cerebral blood flow and metabolism during exercise. Prog Neurobiol 2000;61:397–414. [PubMed: 10727781]

11. Izzetoglu M, Devaraj A, Bunce S, Onaral B. Motion artifact cancellation in NIR spectroscopy using Wiener filtering. IEEE transactions on bio-medical engineering 2005;52:934–8. [PubMed: 15887543]

12. Malonek D, Grinvald A. Interactions between electrical activity and cortical microcirculation revealed by imaging spectroscopy: implications for functional brain mapping. Science 1996;272:551–4. [PubMed: 8614805]

13. Mayhew J, Zheng Y, Hou Y, Vuksanovic B, Berwick J, Askew S, Coffey P. Spectroscopic analysis of changes in remitted illumination: the response to increased neural activity in brain. Neuroimage 1999;10:304–26. [PubMed: 10458944]

14. Mehagnoul-Schipper DJ, van der Kallen BF, Colier WN, van der Sluijs MC, van Erning LJ, Thijssen HO, Oeseburg B, Hoefnagels WH, Jansen RW. Simultaneous measurements of cerebral oxygenation changes during brain activation by near-infrared spectroscopy and functional magnetic resonance imaging in healthy young and elderly subjects. Human brain mapping 2002;16:14–23. [PubMed: 11870923]

15. Mildner T, Norris DG, Schwarzbauer C, Wiggins CJ. A qualitative test of the balloon model for BOLD-based MR signal changes at 3T. Magnetic resonance in medicine 2001;46:891–9. [PubMed: 11675640]

16. Miyai I, Tanabe HC, Sase I, Eda H, Oda I, Konishi I, Tsunazawa Y, Suzuki T, Yanagida T, Kubota K. Cortical mapping of gait in humans: a near-infrared spectroscopic topography study. Neuroimage 2001;14:1186–92. [PubMed: 11697950]

17. Niederhauser BD, Rosenbaum BP, Gore JC, Jarquin-Valdivia AA. A functional near-infrared spectroscopy study to detect activation of somatosensory cortex by peripheral nerve stimulation. Neurocritical care 2008;9:31–6. [PubMed: 17975711]

18. Okamoto M, Dan H, Shimizu K, Takeo K, Amita T, Oda I, Konishi I, Sakamoto K, Isobe S, Suzuki T, et al. Multimodal assessment of cortical activation during apple peeling by NIRS and fMRI. Neuroimage 2004;21:1275–88. [PubMed: 15050555]

19. Perrey S. Non-invasive NIR spectroscopy of human brain function during exercise. Methods 2008;45:289–99. [PubMed: 18539160]

20. Rolfe P. In vivo near-infrared spectroscopy. Annual review of biomedical engineering 2000;2:715–54.

21. Sato H, Fuchino Y, Kiguchi M, Katura T, Maki A, Yoro T, Koizumi H. Intersubject variability of near-infrared spectroscopy signals during sensorimotor cortex activation. Journal of biomedical optics 2005;10:44001. [PubMed: 16178635]

22. Sheth SA, Nemoto M, Guiou M, Walker M, Pouratian N, Toga AW. Linear and nonlinear relationships between neuronal activity, oxygen metabolism, and hemodynamic responses. Neuron 2004;42:347–55. [PubMed: 15091348]

23. Sitaram R, Caria A, Birbaumer N. Hemodynamic brain-computer interfaces for communication and rehabilitation. Neural networks. 2009

24. Sitaram R, Zhang H, Guan C, Thulasidas M, Hoshi Y, Ishikawa A, Shimizu K, Birbaumer N. Temporal classification of multichannel near-infrared spectroscopy signals of motor imagery for developing a brain-computer interface. Neuroimage 2007;34:1416–27. [PubMed: 17196832]

25. Tang L, Avison MJ, Gore JC. Nonlinear blood oxygen level-dependent responses for transient activations and deactivations in V1 - insights into the hemodynamic response function with the balloon model. Magnetic resonance imaging 2009;27:449–59. [PubMed: 18805666]

26. Tomioka H, Yamagata B, Takahashi T, Yano M, Isomura AJ, Kobayashi H, Mimura M. Detection of hypofrontality in drivers with Alzheimer's disease by near-infrared spectroscopy. Neurosci Lett 2009;451:252–6. [PubMed: 19146927]

27. Utsugi, K.; Obata, A.; Sato, H.; Katsura, T.; Sagara, K.; Maki, A.; Koizumi, H. Development of an optical brain-machine interface. Conference proceedings :… Annual International Conference of the IEEE Engineering in Medicine and Biology Society. IEEE Engineering in Medicine and Biology Society. Conference 2007; 2007. p. 5338-41.

28. Villringer A, Chance B. Non-invasive optical spectroscopy and imaging of human brain function. Trends in neurosciences 1997;20:435–42. [PubMed: 9347608]

29. Wilcox T, Bortfeld H, Woods R, Wruck E, Boas DA. Using near-infrared spectroscopy to assess neural activation during object processing in infants. Journal of biomedical optics 2005;10:11010. [PubMed: 15847576]

30. Zhang Q, Brown EN, Strangman GE. Adaptive filtering for global interference cancellation and real-time recovery of evoked brain activity: a Monte Carlo simulation study. Journal of biomedical optics 2007a;12:044014. [PubMed: 17867818]

31. Zhang Q, Brown EN, Strangman GE. Adaptive filtering to reduce global interference in evoked brain activity detection: a human subject case study. Journal of biomedical optics 2007b;12:064009. [PubMed: 18163825]

32. Zhang Q, Strangman GE, Ganis G. Adaptive filtering to reduce global interference in non-invasive NIRS measures of brain activation: how well and when does it work? Neuroimage 2009;45:788–94. [PubMed: 19166945]

33. Zhang Y, Brooks DH, Franceschini MA, Boas DA. Eigenvector-based spatial filtering for reduction of physiological interference in diffuse optical imaging. Journal of biomedical optics 2005;10:11014. [PubMed: 15847580]
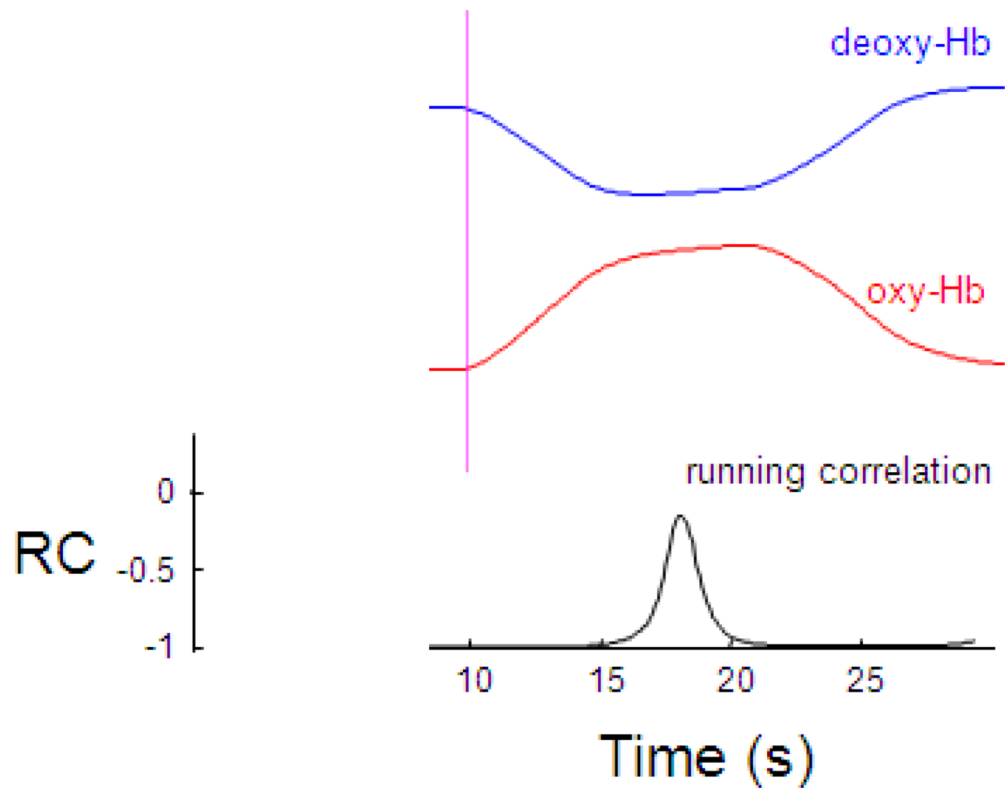
Figure 1.
Oxy-Hb and deoxy-Hb are negatively correlated during neural activation simulated using the Balloon model. Following onset of finger tapping, oxy-Hb (red) increases and deoxy-Hb (blue) decreases. The running correlation (RC) between oxy-Hb and deoxy-Hb is close to −1 but increases when oxy-Hb and deoxy-Hb plateau. The vertical line indicates the onset of finger tapping.
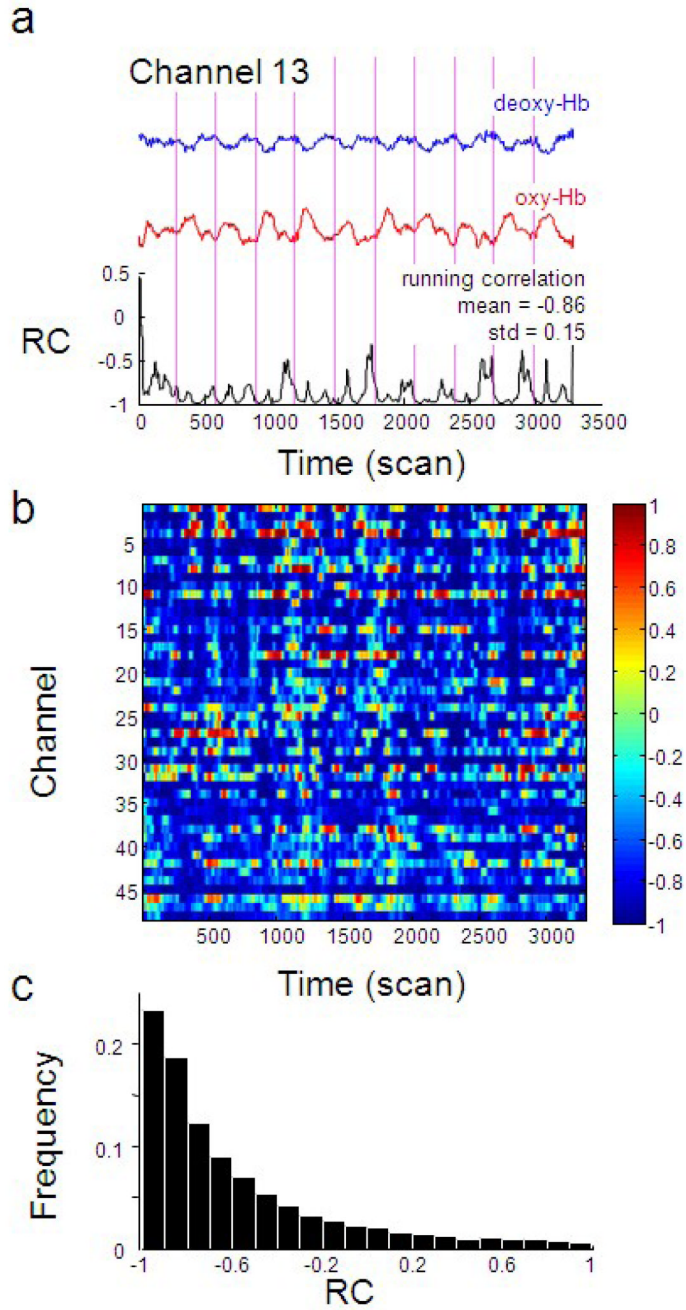
Figure 2.
Oxy-Hb and deoxy-Hb are negatively correlated during finger tapping without head motion.
(a) Time series of oxy-Hb (red), deoxy-Hb (blue) and their running correlation (black) from a
representative channel (channel 13 which corresponds to the left motor cortex) from a single
participant (subject 4). The vertical dotted line indicates the onset of finger tapping. It can be
seen that RC is usually less than −0.5 and often close to −1. (b) Running correlation of all
channels in the same single subject. Each row represents one channel and each column is a
data point (10 data points corresponds to 1s). It can be seen that RC (represented by the color
scale on the right) is largely negative across all channels (mean −0.57, standard deviation 0.43).

(c) The histogram of the distribution of RCs from panel (b) shows the distribution of the running correlation measured above.
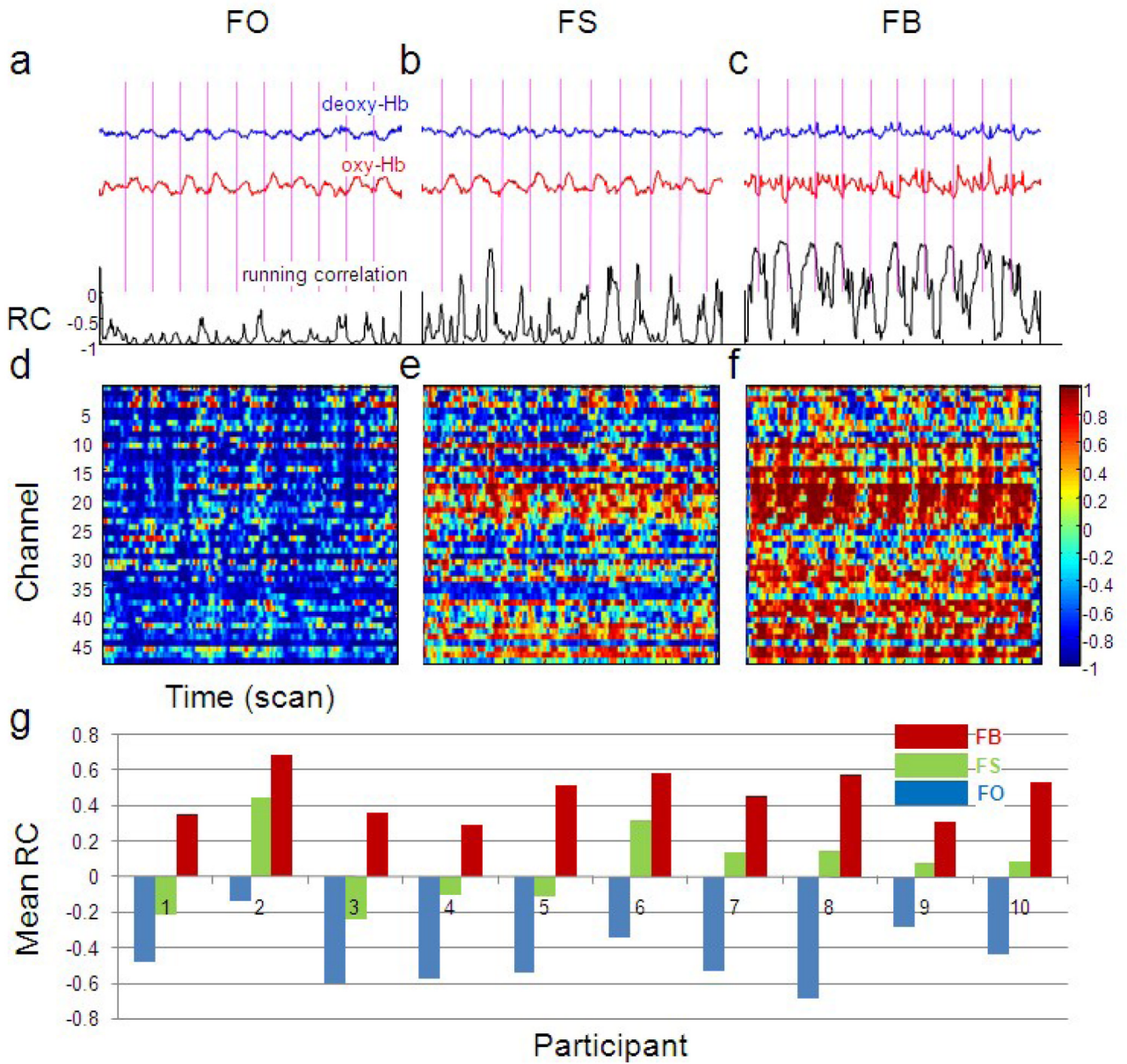
Figure 3.
Head motion induced noise makes the correlation between oxy-Hb and deoxy-Hb higher (less negative). (a), (b) and (c) show the running correlation (black), oxy-Hb (red) and deoxy-Hb (blue) in finger tapping only block (FO), finger tapping with small head motion block (FS), finger tapping with big head motion block (FB), respectively, in channel 13 of subject 4. All time series are on the same scale. The mean RCs are −0.86, −0.62 and 0.10 in the three blocks, respectively. (d), (e) and (f) show the running correlation of subject 4 in the three blocks for all channels. (g) The mean running correlations across channels are shown for all participants in all blocks. The mean increase of running correlation from the FO to FS block is 0.52 (paired T test, df=9, p=3×10^{-6}) across subjects; the increase from the FO to FB block is 0.97 (p=2×10^{-8}).
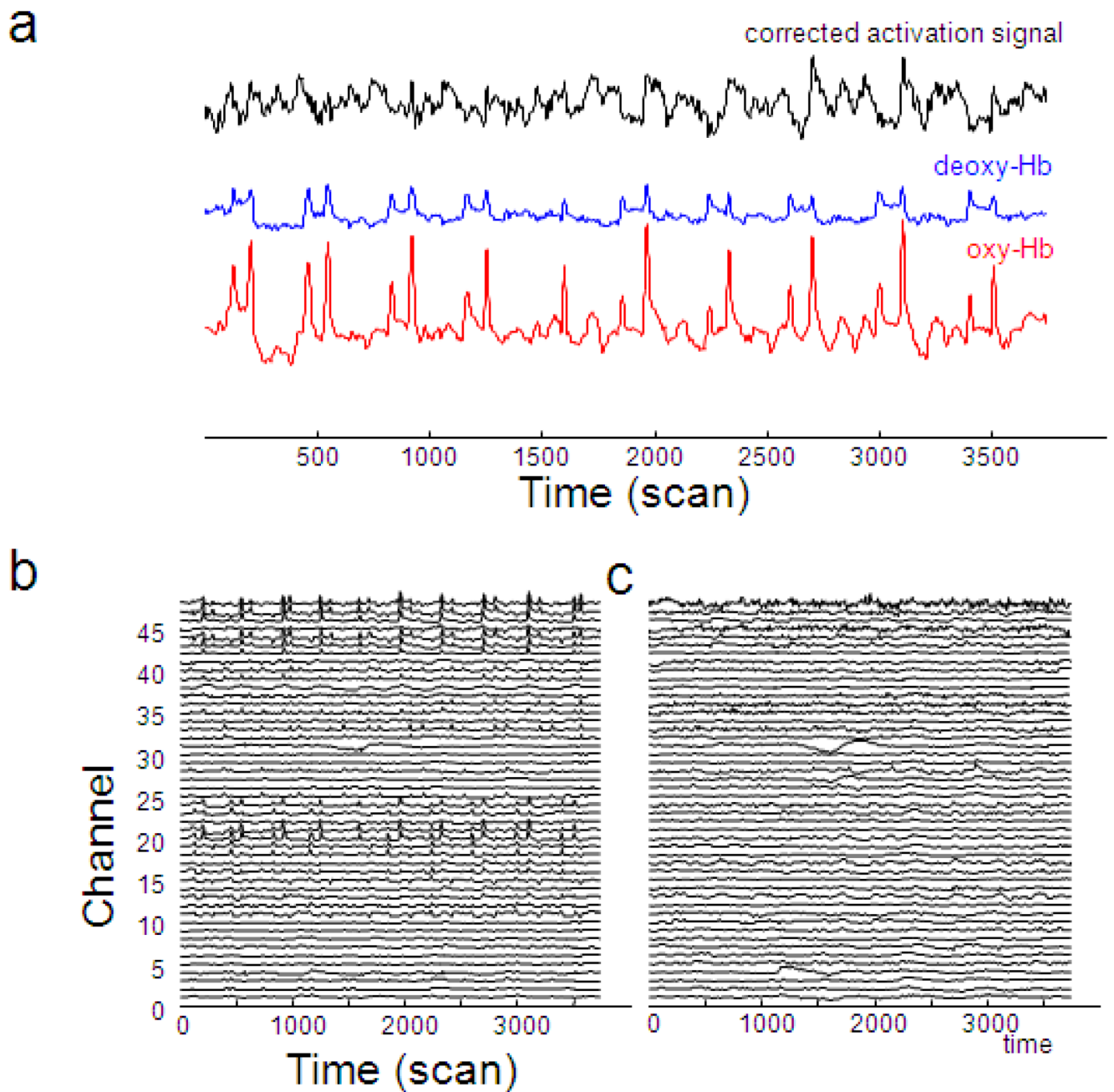
Figure 4.
The CBSI method effectively removes spikes induced by head motion. (a) The original oxy-Hb (red), the original deoxy-Hb (blue), and corrected activation signal (black) from a single channel (channel 24) of subject 4 in block FB. Spikes induced by head motion which are visually evident in both oxy-Hb and deoxy-Hb are largely removed. The original oxy-Hb signal (b) and the corrected activation signal (c) from all channels of subject 4. Each trace is from a single channel. Most spikes are removed by this method.
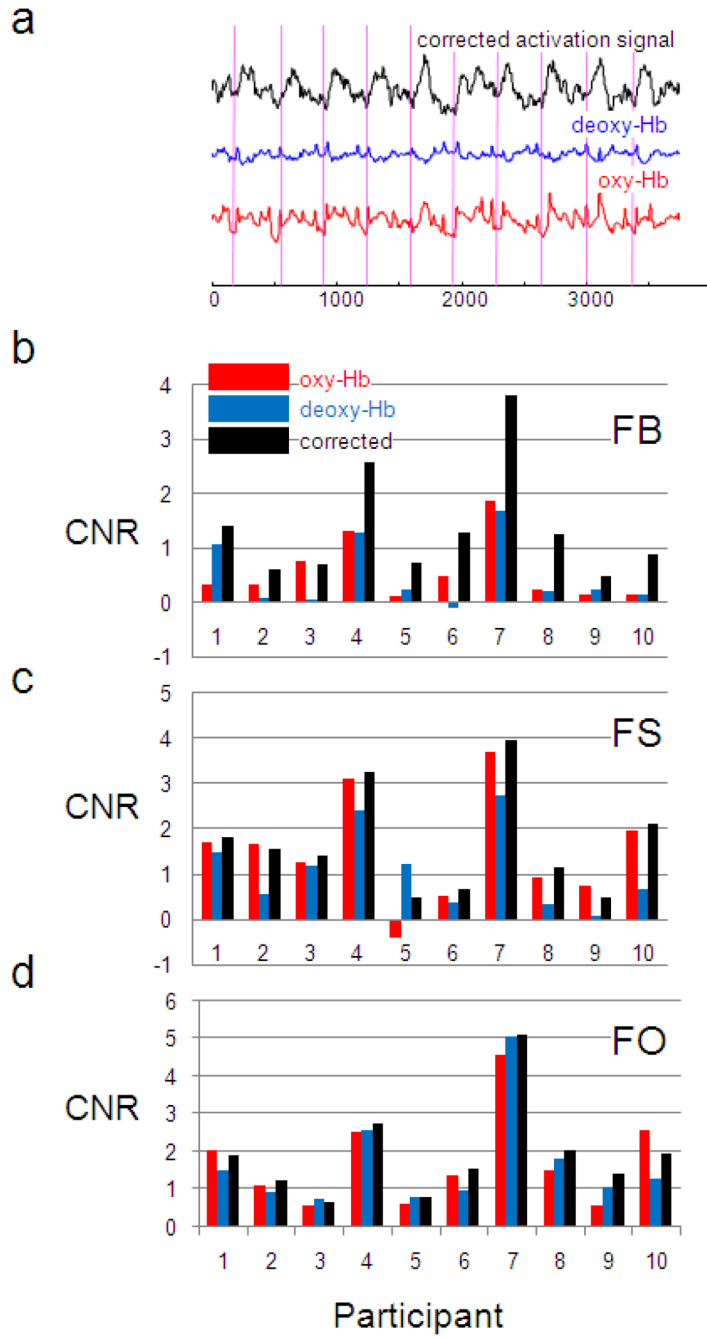
Figure 5.
The CBSI method improves the contrast to noise ratio (CNR). (a) Time series of oxy-Hb (red), deoxy-Hb (blue) and corrected activation signal (black) from channel 13 of subject 4 in the FB block are shown. Vertical lines indicate the onset of finger tapping. Visually, the corrected signal is more correlated to finger tapping than the original signals. (b) CNR of oxy-Hb and deoxy-Hb before and after correction for all subjects in the FB block. Oxy-Hb CNR is improved in 9 of the 10 subjects. The mean improvement is 0.80. Deoxy-Hb CNR is improved for all subjects (mean improvement 0.89). (c) For comparison, CNR before and after correction are plotted in FS and (d) FO blocks. For oxy-Hb, the mean improvement is 0.17 (FS) and 0.21 (FO), both not significant at $p=0.05$; for deoxy-Hb, the mean improvement is 0.59 (FS) and

0.28 (FO), both are significant ($p=3\times10^{-3}$ and 7×10^{-3}, respectively). This smaller CNR improvement in the FO and FS blocks is expected because there is less noise in the original data for this method to remove.
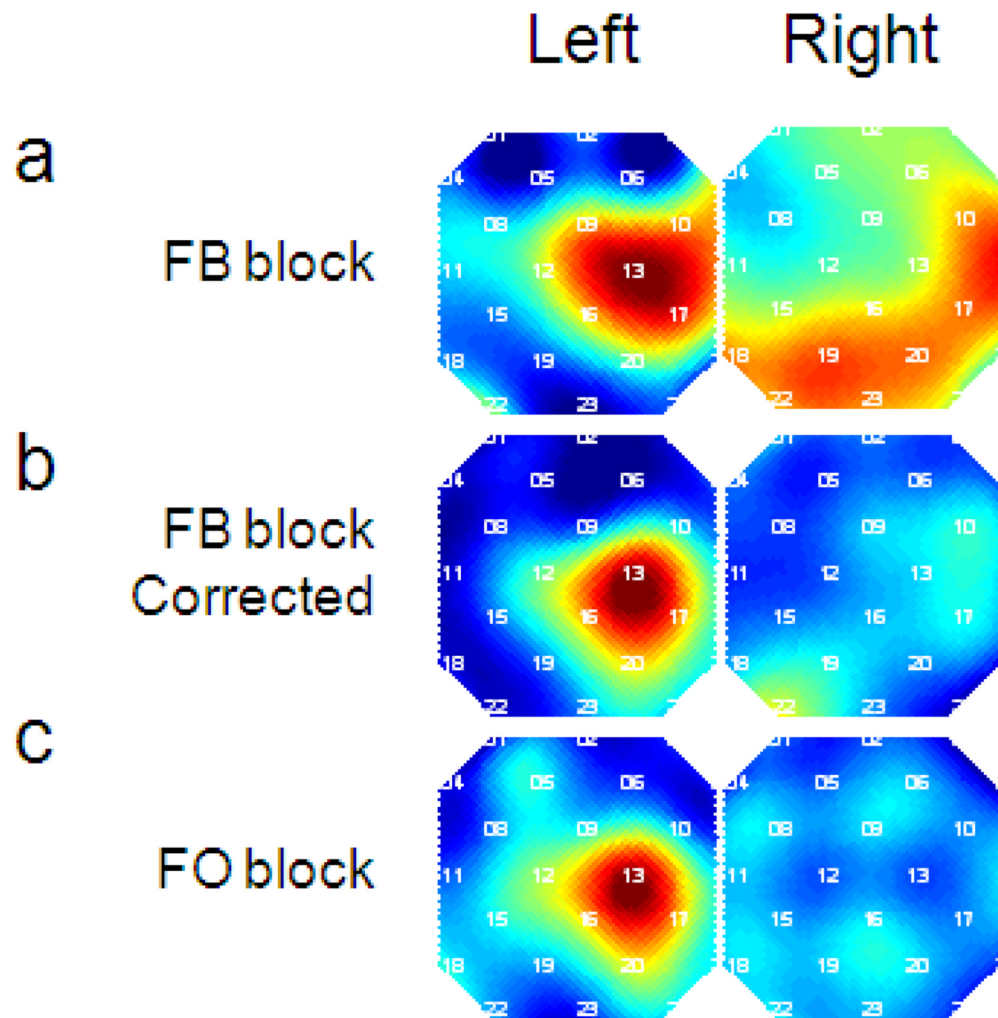
Figure 6.
CBSI method improves the spatial signal quality. (a) CNR map of original oxy-Hb of subject 4 in the FB block. We see that while the contrast correctly localized left motor cortex, the activation is diffuse. (b) CNR map of corrected activation signal for subject 4 in the FB block. Compared to the uncorrected map, the corrected map is much more localized and similar to the map in the FO block (c). The CNR maps are normalized to the maximum and minimum across all channels within each map. Numbers in white indicate the channel number. The spatial maps are smoothed using spline interpolation.
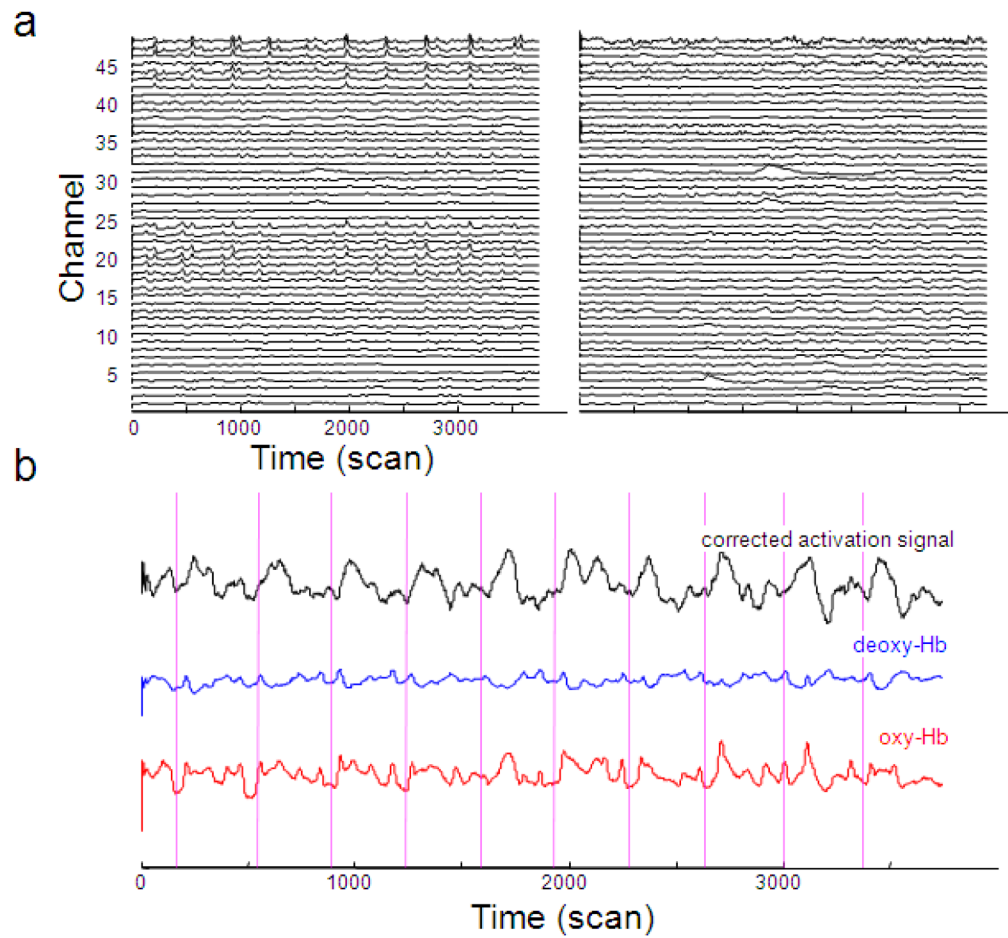
Figure 7.
The CBSI method improves signal quality in real time. (a) The CBSI method removes spikes from the signal (all channels in subject 4). The left panel shows the original oxy-Hb time series and the right panel shows the corrected activation signal. (b) The CBSI method improves signal quality in channel 13 (left motor cortex) in subject 4. The corrected activation signal is more strongly correlated with finger tapping then the original oxy-Hb. Vertical lines indicate the onset of finger tapping blocks.